Importance of the Darrieus-Landau instability for strongly corrugated turbulent flames

Vitaly Bychkov
Institute of Physics, Umeå University, SE–901 87 Umeå, Sweden

(Received 21 February 2003; revised manuscript received 12 August 2003; published 18 December 2003)

The renormalization ideas of self-similar dynamics of a strongly turbulent flame front are applied to the case of a flame with realistically large thermal expansion of the burning matter. In that case a flame front is corrugated both by the external turbulence and by the intrinsic flame instability (the Darrieus-Landau instability). The analytical formulas for the velocity of flame propagation are obtained. It is demonstrated that the flame instability is of principal importance when the maximal hydrodynamic length scale is much larger than the cutoff wavelength of the instability, provided the turbulent intensity is not too high.

DOI: 10.1103/PhysRevE.68.066304 PACS number(s): 47.20.−k, 47.27.−i, 82.33.Vx

I. INTRODUCTION

The role of the hydrodynamic flame instability for premixed turbulent burning in gas turbines and car engines has been widely discussed, but the final answer still remains unknown [1–3]. For a long time it was supposed that the instability influence is minor [1,4]. Now there is mounting evidence that the flame instability is of primary importance for turbulent burning, and sometimes this effect may even dominate [5–11]. For example, the experiments [5,6] demonstrate that flame propagation velocity U_w may increase by a factor of 10 and larger in comparison with the planar flame velocity U_f because of the Darrieus-Landau (DL) instability only. Such a velocity increase is comparable to the velocity observed for turbulent flames [4,12]. The experiments [8] with turbulent flames at different pressures show that flames with the reduced instability effect propagate three to four times slower. Similar tendency may be understood using the following order-of-magnitude reasoning. Turbulent burning in gas turbines and car engines happens typically in the flamelet regime, for which a flame front may be strongly corrugated on large length scales, but it retains the same internal structure as laminar flames [1]. Strictly speaking, the flamelet regime takes place when the planar flame velocity U_f is much larger than the characteristic velocity of turbulent pulsations, $u_{rms}=u_{rms}(\lambda)$, at the length scale equal to the flame thickness, $\lambda=L_f$, that is, $u_{rms}(L_f)/U_f\ll 1$. Thus, the effects of turbulence are relatively small on small length scales $\lambda \simeq L_f$ by definition of the flamelet regime. On large length scales turbulent velocity increases according to the Kolmogorov law $u_{rms}(\lambda)\propto\lambda^{1/3}$, and it may become much larger than the planar flame velocity U_f. However, according to the experiments [5,6] the DL instability leads to a fractal structure of the flame front with the velocity of flame propagation increasing with length scale in the same way, $U_w(\lambda)\propto\lambda^{1/3}$, which implies $u_{rms}(\lambda)/U_w(\lambda)\propto u_{rms}(L_f)/U_f\ll 1$ for all length scales of the gas flow. Of course, the above reasoning is very qualitative, and one needs a more quantitative investigation to understand the role of the DL instability in the flamelet burning regime. Unfortunately, direct numerical simulations cannot help in this case, since the characteristic length scale of the flow, 10–100 cm, exceeds the typical flame thickness, 10^{-4}–10^{-3} cm, by many orders of magnitude. Renormalization analysis [13,14] may work better when such a large number of different length scales is involved in the problem. The original papers [13,14] developed the renormalization ideas in the artificial context of a flame with zero thermal expansion when the densities of the fuel mixture, ρ_f, and the burnt gas, ρ_b, are the same, i.e., the expansion factor $\Theta\equiv\rho_f/\rho_b$ is equal to unity, $\Theta=1$. However, the assumption of $\Theta=1$ is quite far from reality, instead, laboratory and industrial combustion is accompanied by rather strong expansion of burning gaseous mixture, $\Theta=5$–10. As a matter of fact, it is the density drop that causes the DL instability, and the larger is the expansion factor Θ, the stronger is the instability [1,2]. The joint action of the DL instability and the external turbulence has been investigated in Refs. [11,15] on the basis of a model equation in the case of weakly wrinkled flames. It has been obtained in Refs. [11,15] that the flame velocity increase produced by weak turbulence and weak DL instability working together is larger or about the sum of the turbulence effect and the instability effect taken separately.

In the present paper we expand the renormalization ideas of Ref. [14] to the case of a flame front strongly corrugated both by the external turbulence and by the DL instability. Assuming self-similar properties of the corrugated flame dynamics, we find analytical formulas for the propagation velocity of a strongly turbulent flame. We demonstrate that the DL instability is of principal importance when the maximal hydrodynamic length scale is much larger than the cutoff wavelength of the DL instability, provided the turbulent intensity is not too high.

II. STRONGLY CORRUGATED FLAMES PRODUCED BY TURBULENCE ONLY

According to the well-known Clavin-Williams formula [16] obtained in the case of no thermal expansion $\Theta=1$ and zero flame thickness, weak turbulence increases the velocity of a turbulent flame, $\Delta U=U_w-U_f>0$, as

$$\Delta U/U_f=U_{rms}^2/U_f^2, \tag{1}$$

where $U_{rms}=u_{rms}(L_t)$ and L_t is the integral length scale of the turbulent flow. Equation (1) may be also presented with the help of spectral density $\varepsilon_t(k)$ of the turbulent kinetic energy

$$\Delta U/U_f = U_f^{-2} \int_{k_t}^{k_\nu} \varepsilon_t(k)dk, \tag{2}$$

where

$$u_{rms}^2 = \int_k^{k_\nu} \varepsilon_t(\eta)d\eta, \tag{3}$$

$$U_{rms}^2 = \int_{k_t}^{k_\nu} \varepsilon_t(k)dk, \tag{4}$$

$k_t = 2\pi/L_t$ and $k_\nu = 2\pi/L_\nu$ are the wave numbers corresponding to the integral and Kolmogorov (dissipation) length scales L_t and L_ν, the former being usually much larger than the latter $L_t \gg L_\nu$, $k_t \ll k_\nu$. In the case of the Kolmogorov turbulent spectrum $\varepsilon_t(k) \propto k^{-5/3}$ we find from Eq. (3),

$$\varepsilon_t(k) = \frac{2}{3} U_{rms}^2 k_t^{2/3} \left[1 - \left(\frac{k_t}{k_\nu} \right)^{2/3} \right]^{-1} k^{-5/3} \approx \frac{2}{3} U_{rms}^2 k_t^{2/3} k^{-5/3}. \tag{5}$$

Equation (1) has been extrapolated to the case of a strongly turbulent flame assuming self-similar properties of the corrugated front [14]. Following Ref. [14] we decompose the whole spectrum of flame wrinkles into components with different wave numbers (narrow bands in the spectrum), each of them providing a similar small increase of the flame front velocity. Then the first band with the largest possible wave number and the smallest possible length scale increases the flame velocity as $dU_1 = U_{w1} - U_f$,

$$dU_1/U_f = -\varepsilon_t(k_1)dk/U_f^2. \tag{6}$$

The minus sign comes into Eq. (6) because the integral in Eq. (3) is taken from k to k_ν. From the point of view of the second band with the wave number k_2 the value U_{w1} plays the role of the new flame velocity. Then the second band provides the flame velocity increase

$$dU_2/U_{w1} = -\varepsilon_t(k_2)dk/U_{w1}^2, \tag{7}$$

and so on. Let us designate the velocity of flame propagation corresponding to the wrinkles with the wave numbers above k by $U = U(k)$. Since every band in the spectrum of flame wrinkles leads to infinitesimal increase in the flame velocity, we can write Eqs. (6) and (7) in the form

$$dU/U = -\varepsilon_t(k)dk/U^2. \tag{8}$$

Integrating Eq. (8) over the whole turbulent spectrum one obtains the propagation velocity U_w of a strongly corrugated flame with zero thermal expansion $\Theta = 1$ [14],

$$U_w^2 = U_f^2 + 2U_{rms}^2. \tag{9}$$

III. STRONGLY CORRUGATED FLAMES PRODUCED BY THE DL INSTABILITY ONLY

Let us consider similar scale-invariant formulas for the case of a flame front corrugated because of the DL instability only, when there is no external turbulence. It has been obtained experimentally [5,6] that a spherical flame unstable according to the DL mechanism accelerates because of the corrugated structure of the front. The acceleration implies that the velocity of flame propagation, U_w, increases with the maximal characteristic length scale of the hydrodynamic motion, λ_{max}, as

$$U_w = U_f(\lambda_{max}/\lambda_c)^D, \tag{10}$$

where λ_c is the cutoff wavelength of the DL instability proportional to the flame thickness and D is a constant power exponent. The self-similar flame acceleration has been interpreted as development of a fractal structure at the flame front with wrinkles of different wave numbers imposed on each other [5,6]. The theoretical studies of the stability properties of curved flames [3,17,18] lead to similar conclusions. In that case the cutoff wavelength of the DL instability, λ_c, plays the role of the inner cutoff in the fractal cascade and D is the excess of the fractal dimension of the flame front over the embedding dimension (the embedding dimension is 2 for the realistic experiments with three-dimensional flows). According to the experimental measurements [5,6] the fractal excess is approximately $D \approx 1/3$ for all investigated laboratory flames. The theoretical estimates [3,17,18] suggest that the fractal excess depends on the expansion factor $D = D(\Theta)$ with $D \approx 1/3$ for $\Theta = 5$–8, typical for laboratory flames and $D \to 0$ when $\Theta \to 1$. Assuming self-similar properties of the fractal cascade we should expect that the "intermediate" velocity of flame propagation, $U = U(k)$, produced by the wrinkles with wave numbers in between k and $k_c = 2\pi/\lambda_c$ depends on k as

$$U = U_f(k/k_c)^{-D}. \tag{11}$$

The last equation may be also presented in a differential form similar to Eq. (8),

$$dU/U = -\varepsilon_{dl}(k)dk, \tag{12}$$

with $\varepsilon_{dl} = D/k$ for $k_{max} < k < k_c$ and $\varepsilon_{dl} = 0$ when $k \geqslant k_c$. Here k_{max} is the smallest possible wave number allowed by the flow geometry (corresponding to the largest possible wavelength).

IV. THE JOINT EFFECT OF TURBULENCE AND THE DL INSTABILITY FOR A WEAKLY WRINKLED FLAME

When a flame front with realistically large thermal expansion $\Theta = 5$–10 propagates in a turbulent flow, then both the DL instability and the external turbulence contribute to the velocity increase. In the present section we consider the joint effect of the turbulence and the instability for a weakly wrinkled flame. In general, the velocity increase depends both on the scaled turbulent intensity U_{rms}^2/U_f^2 and on the intrinsic parameters of flame dynamics such as Θ, the flow geometry, etc.:

$$\Delta U/U_f = F(U_{rms}^2/U_f^2, \Theta, \ldots). \tag{13}$$

When turbulence is weak $U_{rms}^2/U_f^2 \ll 1$, the last formula may be reduced to

$$\Delta U/U_f \approx C_{dl} + C_t U_{rms}^2/U_f^2, \tag{14}$$

with the factors C_{dl} and C_t depending on intrinsic flame parameters. Obviously, the term C_{dl} specifies the velocity increase of a flame front due to the DL instability only, when turbulent intensity is zero $U_{rms}^2/U_f^2 = 0$,

$$(\Delta U/U_f)_{dl} = C_{dl}. \tag{15}$$

This increase has been investigated in a large number of papers; see the analytical theory [19], the direct numerical simulations [18,20,21], and the recent review [3]. The velocity increase results from the balance between the DL instability, the thermal stabilization, and the nonlinear geometrical (Huygens) stabilization. The effect of Huygens stabilization is also similar to kinematic restoration of turbulent flames described in Ref. [10]. In both cases corrugations of the front (produced either by instability or by turbulence) are ''removed'' by local flame propagation. As a matter of fact, both Huygens stabilization and kinematic restoration are produced by the same term of nonlinear equations describing flame dynamics. For example, within the scope of the approach of Ref. [10], the stabilization/restoration is related to the first term on the right-hand side of Eq. (7) of Ref. [10].

At present there is not so much information about the second factor C_t of Eq. (14). Comparing Eq. (14) and the Clavin-Williams formula, Eq. (1), we can say for sure that $C_t = 1$ for $\Theta = 1$ (we also have $C_{dl} = 0$ in the same limit of $\Theta = 1$). According to the model studies [11,15], the factor C_t may be evaluated from below by the respective coefficient of the turbulence-induced solution of the flame equations, which is not influenced by the DL instability directly. The main idea of the turbulence-induced solution may be explained in the following way. Suppose that dynamics of a weakly wrinkled flame front $z = f(\mathbf{x},t) - U_w t$ in an external turbulent flow u_z may be described by an equation

$$\hat{\mathcal{L}} f + \frac{\Delta U}{U_f} - \hat{\mathcal{N}}_1(f,f) - \hat{\mathcal{N}}_2(u_z,f) - \hat{\mathcal{N}}_3(u_z,u_z) = \hat{\mathcal{L}}_t u_z, \tag{16}$$

where $\hat{\mathcal{L}}$, $\hat{\mathcal{L}}_t$ are linear operators and $\hat{\mathcal{N}}_1$, $\hat{\mathcal{N}}_2$, $\hat{\mathcal{N}}_3$ are nonlinear operators of the second order. For example, the effect of kinematic restoration of a weakly wrinkled front originates from a nonlinear operator $\hat{\mathcal{N}}(f,f) \propto \nabla f \cdot \nabla f = (\nabla f)^2$. We are interested in the dynamics of a statistically stationary flame front in the reference frame of the front, therefore we have added the velocity increase $\Delta U/U_f$ directly into the equation. Choosing another reference frame we would have $\Delta U/U_f$ included in the first time derivative of the front position. In fact, to derive an equation like Eq. (16) is a difficult task by itself, which has not been fulfilled yet. So far such an equation has been obtained only in some limiting cases, given as follows.

(1) In the artificial case of zero thermal expansion $\Theta = 1$, Eq. (16) coincides with the G equation proposed in Ref. [22] and written for a weakly wrinkled flame.

(2) When thermal expansion is nonzero but ultimately weak, $\Theta - 1 \ll 1$, and turbulence is zero, then Eq. (16) goes over to the Sivashinsky equation [23]. Turbulence may be included into the Sivashinsky equation similar to Ref. [9].

(3) In the linear case of small amplitude of flame wrinkles, Eq. (16) reproduces the dispersion relation of the DL instability [24] and linear response of a flame front to external turbulence [25]. In that case Eq. (16) takes the form

$$\hat{\mathcal{L}} f = 0 \tag{17}$$

and

$$\hat{\mathcal{L}} f = \hat{\mathcal{L}}_t u_z, \tag{18}$$

respectively. The theories [24,25] have been developed for realistically large thermal expansion of burning matter.

(4) For curved stationary flames with realistically large thermal expansion, Eq. (16) reproduces the nonlinear equation derived in Ref. [19]. In that case Eq. (16) is

$$\hat{\mathcal{L}} f + \frac{\Delta U}{U_f} - \hat{\mathcal{N}}_1(f,f) = 0. \tag{19}$$

(5) An attempt to derive a similar nonstationary nonlinear equation led to a rather cumbersome result [17]; therefore, subsequent studies of weakly turbulent flames subject to the DL instability [11,15] have been performed on the basis of a model equation [26], which is not rigorous but has a relatively simple form.

Still, in the present paper a particular form of Eq. (16) is not important. What is important is that Eq. (16) describes a weakly wrinkled turbulent flame and takes into account the DL instability. The turbulent velocity in Eq. (16) may be specified as a combination of Fourier harmonics with random phases similar to Ref. [9]. For example, in the case of a two-dimensional incompressible ''stationary'' flow considered in Ref. [9] the turbulent velocity u_z may be presented in the laboratory reference frame as

$$u_z = \sum U_i \cos(k_i x + \varphi_{ix}) \cos(k_i z + \varphi_{iz}), \tag{20}$$

where the amplitudes U_i obey the Kolmogorov spectrum. In the reference frame of the propagating flame front the turbulent velocity u_z is strongly oscillating,

$$u_z = \sum U_i \cos(k_i x + \varphi_{ix}) \cos(k_i U_w t + \varphi_{iz}), \tag{21}$$

which leads to a particular strongly oscillating turbulence-induced solution to Eq. (18) in the form

$$f = \sum f_i \cos(k_i x + \varphi_{ix}) \cos(k_i U_w t + \varphi_{iz} + \Delta\varphi_i). \tag{22}$$

Here $\Delta\varphi_i$ is the phase shift in time with respect to the velocity oscillations (21).

In general, both the DL instability and the turbulence contribute to the solution to Eq. (16). However, as was shown in Refs. [3,11,15,19], the instability working alone leads to a stationary (or quasistationary) solution, while the turbulence-induced solution is strongly oscillating. Therefore, it would be reasonable to look for a solution to Eq. (16) in the form of superposition of a stationary part and a strongly oscillating part:

$$f = g(\mathbf{x}) + h(\mathbf{x},t). \tag{23}$$

Substituting Eq. (23) into Eq. (16) we find

$$\hat{\mathcal{L}}g + \hat{\mathcal{L}}h + \frac{\Delta U}{U_f} - \hat{\mathcal{N}}_1(g,g) - \hat{\mathcal{N}}_1(g,h) - \hat{\mathcal{N}}_1(h,g) - \hat{\mathcal{N}}_1(h,h) - \hat{\mathcal{N}}_2(u_z,g) - \hat{\mathcal{N}}_2(u_z,h) - \hat{\mathcal{N}}_3(u_z,u_z) = \hat{\mathcal{L}}_t u_z. \tag{24}$$

We separate the stationary and oscillating terms in Eq. (24) by taking time average, $\langle \cdots \rangle_\tau$,

$$\hat{\mathcal{L}}g + \frac{\Delta U}{U_f} - \hat{\mathcal{N}}_1(g,g) - \langle \hat{\mathcal{N}}_1(h,h)\rangle_\tau - \langle \hat{\mathcal{N}}_2(u_z,h)\rangle_\tau - \langle \hat{\mathcal{N}}_3(u_z,u_z)\rangle_\tau = 0 \tag{25}$$

and subtracting Eq. (25) from Eq. (24),

$$\hat{\mathcal{L}}h - \hat{\mathcal{N}}_1(g,h) - \hat{\mathcal{N}}_1(h,g) - \hat{\mathcal{N}}_1(h,h) + \langle \hat{\mathcal{N}}_1(h,h)\rangle_\tau - \hat{\mathcal{N}}_2(u_z,g) - \hat{\mathcal{N}}_2(u_z,h) + \langle \hat{\mathcal{N}}_2(u_z,h)\rangle_\tau - \hat{\mathcal{N}}_3(u_z,u_z) + \langle \hat{\mathcal{N}}_3(u_z,u_z)\rangle_\tau = \hat{\mathcal{L}}_t u_z. \tag{26}$$

In the case of weak nonlinearity we can neglect the nonlinear terms in Eq. (26), which leads to the linear equation (18) written for the value h and specifies the turbulence-induced solution

$$h = \hat{\mathcal{L}}^{-1}\hat{\mathcal{L}}_t u_z. \tag{27}$$

If for some reason the DL instability does not develop, $g = 0$, then the flame velocity in Eq. (25) increases because of the turbulence-induced solution only:

$$\left(\frac{\Delta U}{U_f}\right)_{g=0} = \langle \hat{\mathcal{N}}_1(h,h)\rangle + \langle \hat{\mathcal{N}}_2(u_z,h)\rangle + \langle \hat{\mathcal{N}}_3(u_z,u_z)\rangle \equiv \left(\frac{\Delta U}{U_f}\right)_t, \tag{28}$$

where $\langle \cdots \rangle$ stands for complete averaging. In general, in order to find the velocity increase we have to solve the eigenvalue problem (25) with the function $\langle \hat{\mathcal{N}}_1(h,h)\rangle_\tau + \langle \hat{\mathcal{N}}_2(u_z,h)\rangle_\tau + \langle \hat{\mathcal{N}}_3(u_z,u_z)\rangle_\tau$ determined by the external turbulence. The eigenvalue problem is similar to the problem of the velocity increase for curved stationary flames; see Eq. (19) and Ref. [19]. In the absence of turbulence, when $u_z = 0$, $h = 0$, Eq. (25) describes the shape of a stationary flame front $z = g_0(\mathbf{x})$ curved because of the DL instability only with the velocity of flame propagation

$$\left(\frac{\Delta U}{U_f}\right)_{h=0} = \langle \hat{\mathcal{N}}_1(g_0,g_0)\rangle \equiv \left(\frac{\Delta U}{U_f}\right)_{dl}, \tag{29}$$

When $h \neq 0$, then the terms $\langle \hat{\mathcal{N}}_1(h,h)\rangle_\tau + \langle \hat{\mathcal{N}}_2(u_z,h)\rangle_\tau + \langle \hat{\mathcal{N}}_3(u_z,u_z)\rangle_\tau$ affect the solution to Eq. (25) and we have the velocity increase

$$\frac{\Delta U}{U_f} = \langle \hat{\mathcal{N}}_1(g,g)\rangle + \langle \hat{\mathcal{N}}_1(h,h)\rangle + \langle \hat{\mathcal{N}}_2(u_z,h)\rangle + \langle \hat{\mathcal{N}}_3(u_z,u_z)\rangle, \tag{30}$$

where g may be different from g_0. We are interested in the case where g and h are of the same order of magnitude, and the flame is weakly wrinkled, that is $\Delta U/U_f \ll 1$, $\langle \hat{\mathcal{N}}_1(g,g)\rangle \ll 1$, $\langle \hat{\mathcal{N}}_1(h,h)\rangle \ll 1$, $\langle \hat{\mathcal{N}}_2(u_z,h)\rangle \ll 1$, $\langle \hat{\mathcal{N}}_3(u_z,u_z)\rangle \ll 1$. Then the terms $\langle \hat{\mathcal{N}}_1(h,h)\rangle_\tau + \langle \hat{\mathcal{N}}_2(u_z,h)\rangle_\tau + \langle \hat{\mathcal{N}}_3(u_z,u_z)\rangle_\tau$ induce a particular solution to Eq. (25),

$$\hat{\mathcal{L}}g_p = \langle \hat{\mathcal{N}}_1(h,h)\rangle_\tau - \langle \hat{\mathcal{N}}_1(h,h)\rangle + \langle \hat{\mathcal{N}}_2(u_z,h)\rangle_\tau - \langle \hat{\mathcal{N}}_2(u_z,h)\rangle + \langle \hat{\mathcal{N}}_3(u_z,u_z)\rangle_\tau - \langle \hat{\mathcal{N}}_3(u_z,u_z)\rangle, \tag{31}$$

which leads to negligibly small terms of the third order and higher, when substituted into the operator $\hat{\mathcal{N}}_1(g,g)$. In that case the solution to Eq. (25) takes the form $g = g_0 + g_p$ with the velocity increase

$$\frac{\Delta U}{U_f} = \langle \hat{\mathcal{N}}_1(g_0,g_0)\rangle + \langle \hat{\mathcal{N}}_1(h,h)\rangle + \langle \hat{\mathcal{N}}_2(u_z,h)\rangle + \langle \hat{\mathcal{N}}_3(u_z,u_z)\rangle, \tag{32}$$

that is,

$$\frac{\Delta U}{U_f} = \left(\frac{\Delta U}{U_f}\right)_{dl} + \left(\frac{\Delta U}{U_f}\right)_t. \tag{33}$$

The above reasoning is supported by the results of the nonlinear models [11,15] in the limit of a weakly wrinkled flame, $\Delta U/U_f \ll 1$.

Comparing Eqs. (14) and (33) we can see that the factor C_t may be evaluated by the respective coefficient found for the turbulence-induced solution. The turbulence-induced solution has been obtained recently ''from the first principles'' for the case of an infinitely thin flame front [27]:

$$C_t = \frac{16\Theta^3}{(\Theta+1)[4\Theta^2 + (\Theta^2+1)^2]}. \tag{34}$$

In the artificial limit of zero thermal expansion $\Theta = 1$ we find $C_t = 1$ from Eq. (34). In the domain of realistically large thermal expansion the coefficient C_t decreases with Θ, and for $\Theta = 5$–8, typical for methane or propane flames the formula, Eq. (34) gives $C_t = 0.25$–0.45. It is curious that the

velocity increase provided by the turbulence-induced solution is smaller for larger thermal expansion, which is opposite to the qualitative properties of the DL instability. It is well known that larger thermal expansion leads to stronger DL instability with larger velocity of flame propagation [3,19]. Different flame behavior in these two cases may be explained in the following way. The DL instability develops because of the flame interaction with the flow, and the larger is the expansion factor Θ, the stronger is the interaction leading to stronger instability. On the contrary, when we study the turbulence-induced solution, then the same interaction plays the role of inertia. In that case the flame-flow interaction generates potential modes in the fuel mixture and in the burnt matter at the expense of the turbulent energy, and reduces the effect of turbulence on the flame front. Since the flame-flow interaction is stronger at larger Θ, the result of the turbulence-induced solution becomes weaker at larger thermal expansion in agreement with Eq. (34). To illustrate the above tendency we would also like to mention that stabilization of the DL instability by acoustic waves increases strongly the amplitude of the turbulence-induced solution [28]. The resonance of the turbulence-induced harmonic with the wavelength equal to the cutoff wavelength of the DL instability, $\lambda=\lambda_c$, obtained in Ref. [25] is another manifestation of the same tendency.

Still, the model analysis [11,15] shows that finite flame thickness may increase the coefficient C_t noticeably in comparison with Eq. (34). One more effect, which has not been taken into account in reasoning (23)–(33), is fast propagation of a flame front along the vortex axis. This is a nonlinear effect related to nonzero thermal expansion [29], which also contributes to the flame velocity increase in an external turbulent flow. Thus, since the theory of weakly curved turbulent flames is not completed yet, in what follows it would be reasonable to treat C_t as a factor of order of unity.

V. THE EXTERNAL TURBULENCE AND THE DL INSTABILITY WORK TOGETHER FOR STRONGLY CORRUGATED FLAMES

Taking into account the velocity increase for a weakly wrinkled flame, Eqs. (14) and (15), and assuming self-similar properties of a flame front at different length scales we can find the velocity of a strongly corrugated flame influenced both by the external turbulence and the DL instability. On the basis of Eqs. (8) and (12) the velocity increase produced by one narrow band in the turbulent spectrum may be written as

$$dU/U=-\varepsilon_{dl}(k)dk-C_t\frac{\varepsilon_t(k)}{U^2}dk \tag{35}$$

or

$$\frac{1}{2}\frac{d}{dk}(U^2)=-\varepsilon_{dl}(k)U^2-C_t\varepsilon_t(k), \tag{36}$$

where the term $\varepsilon_{dl}=D/k$ for $k_{max}<k<k_c$ is related to the DL instability and ε_t is the spectrum of turbulent energy, which is nonzero for $k_t<k<k_\nu$. Thus we come to a linear differential equation with coefficients depending on the variable, Eq. (36), which may be solved analytically by a standard method. Still the solution to Eq. (36) takes different forms for different values of the problem parameters D, k_{max}, k_t, k_c, k_ν, and U_{rms}/U_f. Not all of these parameters may be varied independently in a combustion experiment. Particularly, the geometry of the burning chamber usually determines the integral turbulent length scale L_t, the maximal hydrodynamic length scale λ_{max}, and the respective wave numbers $k_t=2\pi/L_t$, $k_{max}=2\pi/\lambda_{max}$ with $k_{max}\leqslant k_t$. The integral length scale may be equal to the maximal length scale when turbulence is produced directly by the walls of the burning chamber. On the contrary, the integral length scale is smaller than the maximal length scale when the flow involves a special contraption (grid, fans, etc.) intended to break large scale eddies into smaller ones. An example of such a flow may be found in Ref. [34]. Parameters of the fuel mixture specify the planar flame velocity and thickness, U_f and L_f, as well as the DL cutoff wave number $k_c\propto L_f^{-1}$ and the fractal excess D. On the contrary, the Kolmogorov cutoff wave number k_ν depends on the turbulent intensity via the turbulent Reynolds number $k_\nu/k_t=\mathrm{Re}^{3/4}$, where the Reynolds number is defined as $\mathrm{Re}=U_{rms}L_t/\nu$, and ν is the kinematic viscosity [30]. Taking into account the relation between the planar flame parameters $U_fL_f=\nu_{th}=\nu/\mathrm{Pr}$, where ν_{th} is thermal diffusivity and Pr is the Prandtl number, we may present the Reynolds number in the form $\mathrm{Re}=(U_{rms}L_t)/(PrU_fL_f)$. Then the Kolmogorov cutoff wave number may be evaluated as

$$k_\nu=k_t\left(\frac{U_{rms}L_t}{PrU_fL_f}\right)^{3/4}. \tag{37}$$

For fixed parameters of the burning chamber and the fuel mixture we get smaller Kolmogorov cutoff wave number for smaller turbulent intensity. Still k_ν cannot be smaller than k_t since turbulence decays for $\mathrm{Re}<1$. Below, we will consider the case of very large turbulent length scales $k_t\ll k_c$, $k_t\ll k_\nu$ and different relations between the DL cutoff k_c and the Kolmogorov cutoff k_ν, which depends on the turbulent intensity.

A. $k_\nu<k_c$

First, we consider intermediate wave numbers $k_\nu>k>k_t\geqslant k_{max}$. Solution to Eq. (36) may be written as

$$U^2=C_1\left(\frac{k}{k_c}\right)^{-2D}+2C_tk^{-2D}\int_k^{k_\nu}\eta^{2D}\varepsilon_t(\eta)d\eta, \tag{38}$$

where the integration constant is $C_1=U_f^2$, since at short wavelengths $k>k_c>k_\nu$ the DL instability is suppressed by thermal conduction, there is no external turbulence, and we have $U=U_f$ at $k=k_c$. Keeping in mind the expression for the spectral density $\varepsilon_t(k)$ of the Kolmogorov turbulent kinetic energy and assuming a broad turbulent spectrum with $L_t\gg\lambda_c$ we find different solutions (38) for different values of the fractal excess $D<1/3$, $D=1/3$, and $D>1/3$. When $D\neq1/3$, then solution (38) is

$$U^2=U_f^2\left(\frac{k}{k_c}\right)^{-2D}+\frac{2C_tU_{rms}^2}{3D-1}\times\left[1-\left(\frac{k_t}{k_\nu}\right)^{2/3}\right]^{-1}\left(\frac{k}{k_t}\right)^{-2/3}\left[\left(\frac{k_\nu}{k}\right)^{2D-2/3}-1\right]. \quad (39)$$

Below, we take $k\ll k_\nu$, which is the most interesting in practice. Then in the case of small fractal excess $D<1/3$ we obtain from Eq. (39)

$$U^2=U_f^2\left(\frac{k}{k_c}\right)^{-2D}+\frac{2C_t}{1-3D}U_{rms}^2\left(\frac{k}{k_t}\right)^{-2/3} \quad (40)$$

or

$$U^2=U_f^2\left(\frac{k}{k_c}\right)^{-2D}+\frac{2C_t}{1-3D}u_{rms}^2, \quad (41)$$

since $u_{rms}^2=U_{rms}^2(k/k_t)^{-2/3}$. Taking $k=k_{max}\leqslant k_t$ we come to the formula for the turbulent flame velocity produced by the whole spectrum of wrinkles:

$$U_w^2=U_f^2\left(\frac{\lambda_{max}}{\lambda_c}\right)^{2D}+\frac{2C_t}{1-3D}U_{rms}^2. \quad (42)$$

The above result obviously reproduces the Pocheau formula (9) in the limit of no thermal expansion $\Theta=1$ with no influence of the DL instability when $D=0$ and $C_t=1$. When Θ is large and the DL instability influences flame dynamics, then the velocity of flame propagation, Eq. (42), is larger than Eq. (9) for two reasons: the first term on the right-hand side increases by the fractal-related factor $(\lambda_{max}/\lambda_c)^{2D}$ and the second term increases by the factor $(1-3D)^{-1}$, which comes due to the coupling of the instability and the external turbulence.

In the case of large fractal excess $D>1/3$ solution (39) is

$$U^2=U_f^2\left(\frac{k}{k_c}\right)^{-2D}+\frac{2C_t}{3D-1}u_{rms}^2\left(\frac{k}{k_\nu}\right)^{-2D+2/3} \quad (43)$$

for an intermediate wave number $k_\nu\gg k>k_t$ and

$$U_w^2=U_f^2\left(\frac{\lambda_{max}}{\lambda_c}\right)^{2D}+\frac{2C_t}{3D-1}U_{rms}^2\left(\frac{L_t}{L_\nu}\right)^{2D-2/3} \quad (44)$$

for the whole spectrum of flame wrinkles.

The parameter value $D=1/3$ is special for Eq. (38) with the Kolmogorov spectrum of external turbulence $\varepsilon_t(k)\propto k^{-5/3}$. At the same time $D=1/3$ is the most interesting from the point of view of the experimental results [5,6]. Taking $D=1/3$ we obtain from Eq. (38) that

$$U^2=U_f^2\left(\frac{k}{k_c}\right)^{-2/3}+\frac{4}{3}C_tU_{rms}^2\left(\frac{k}{k_t}\right)^{-2/3}\ln(k_\nu/k), \quad (45)$$

or

$$U^2=U_f^2\left(\frac{k}{k_c}\right)^{-2/3}+\frac{4}{3}C_tu_{rms}^2\ln(k_\nu/k). \quad (46)$$

For the whole spectrum of flame wrinkles we find the velocity of flame propagation,

$$U_w^2=U_f^2\left(\frac{\lambda_{max}}{\lambda_c}\right)^{2/3}+\frac{4}{3}C_tU_{rms}^2\ln(L_t/L_\nu). \quad (47)$$

When turbulent intensity is zero $U_{rms}=0$, then Eq. (47) goes over to the velocity increase produced by the DL instability only, Eq. (10). Using the relation between the turbulent and Kolmogorov length scales $L_t/L_\nu=\mathrm{Re}^{3/4}$ we may also present Eq. (47) in the form

$$U_w^2=U_f^2\left(\frac{\lambda_{max}}{\lambda_c}\right)^{2/3}+C_t\ln(\mathrm{Re})U_{rms}^2. \quad (48)$$

Comparing the second terms in the velocity increase in Eqs. (9) and (48) (the terms related to the external turbulence) we can see that the turbulent term in Eq. (48) is multiplied by a large factor $\ln\mathrm{Re}\gg 1$, which makes the effect of external turbulence much stronger in the presence of the strong DL instability.

B. $k_\nu>k_c$

The case of $k_\nu>k_c$ is more typical for combustion experiments than the opposite situation $k_\nu<k_c$ studied in the preceding section. In the case of $k_\nu>k_c$ we have to consider separately two domains of large and small wave numbers (short and long wavelengths), $k_c<k<k_\nu$ and $k_t<k<k_c$, respectively. When the wave numbers of flame wrinkles are larger than the DL cutoff, $k_c<k<k_\nu$, then one should expect from Eq. (35) that the velocity of flame propagation increases because of the external turbulence only. However, it has been shown in Refs. [11,15,25] that flame response to external turbulence is quite different for large and small wave numbers. In the case of a wave number larger than the DL cutoff, $k>k_c$ (small length scales), thermal conduction suppresses strongly all wrinkles at the flame front, and the assumption of a self-similar flame behavior breaks down. This conclusion is also supported by the experiments [25,31–33]. Particularly, according to Ref. [32], the inner cutoff wavelength in the spectrum of flame wrinkles is almost independent of turbulent intensity expressed by use of the Karlovitz number in a rather large domain $0.1<\mathrm{Ka}<10$. Instead, the inner cutoff wavelength is equal approximately $(10-40)L_f$ for different fuel mixtures, which is well correlated with the typical cutoff wavelength of the DL instability $\lambda_c=(20-50)L_f$ [1–3,24,25]. Because of the strong thermal suppression, the harmonics of external turbulence with large wave numbers $k>k_c$ (small wavelength $\lambda<\lambda_c$) wrinkle the flame front only slightly and produce almost no increase in the flame velocity $U(k_c)\approx U_f$. Of course, such a conclusion holds only for moderate turbulent intensity. Increasing the turbulent intensity we may produce strong wrinkling of the flame front even at large wave numbers $k>k_c$, but in that case turbulence works against thermal conduction modifying the inner structure of the flame front. However, when the inner flame structure is modified, we go over from

the flamelet regime of turbulent burning to the regime of thickened flames, which is beyond the scope of the present paper.

For small wave numbers $k_t<k<k_c$ (large wavelengths $L_t>\lambda>\lambda_c$) the solution to Eq. (36) is

$$U^2=C_2\left(\frac{k}{k_c}\right)^{-2D}+2C_t k^{-2D}\int_k^{k_c}\eta^{2D}\varepsilon_t(\eta)d\eta, \quad (49)$$

where the integration constant is $C_2=U^2(k_c)\approx U_f^2$, since the velocity of flame propagation at $k=k_c$ is approximately equal to the planar flame velocity. Then we may write the solution, Eq. (49) similar to that in Sec. IV A replacing k_ν by k_c. Particularly, the counterparts of formulas (39), (42), (44), and (47) are

$$U^2=U_f^2\left(\frac{k}{k_c}\right)^{-2D}+\frac{2C_tU_{rms}^2}{3D-1}\times\left[1-\left(\frac{k_t}{k_\nu}\right)^{2/3}\right]^{-1}\left(\frac{k}{k_t}\right)^{-2/3}\left[\left(\frac{k_c}{k}\right)^{2D-2/3}-1\right] \quad (50)$$

for $D\neq 1/3$,

$$U_w^2=U_f^2\left(\frac{\lambda_{max}}{\lambda_c}\right)^{2D}+\frac{2C_t}{1-3D}U_{rms}^2 \quad (51)$$

for $D<1/3$, $k_c\gg k_t$,

$$U_w^2=U_f^2\left(\frac{\lambda_{max}}{\lambda_c}\right)^{2D}+\frac{2C_t}{3D-1}U_{rms}^2\left(\frac{L_t}{\lambda_c}\right)^{2D-2/3} \quad (52)$$

for $D>1/3$, $k_c\gg k_t$, and

$$U_w^2=U_f^2\left(\frac{\lambda_{max}}{\lambda_c}\right)^{2/3}+\frac{4}{3}C_tU_{rms}^2\ln(L_t/\lambda_c) \quad (53)$$

for $D=1/3$.

VI. RESULTS AND DISCUSSION

The most illustrative way to present the formulas, Eqs. (51)–(53), in a figure is to plot square of the flame velocity versus square of the turbulent velocity. In that case we have a family of straight lines depending on the problem parameters. For example, Fig. 1 illustrates the dependence of the flame propagation velocity on the turbulent intensity for different values of the integral turbulent length scale $\lambda_{max}/\lambda_c=10$, 50, and 100. To be particular, in Fig. 1 we have chosen $L_t=\lambda_{max}$ and the fractal excess of the unstable laminar flame front $D=1/3$ similar to the experimental results [5,6]. As we can see in the figure, the larger are the maximal hydrodynamic length scale and the turbulent length scale, the larger is the velocity of flame propagation. An important point of all plots is that when turbulent intensity is zero, $U_{rms}=0$, the velocity of flame propagation, U_w, is still different from the planar flame velocity U_f. This effect happens because of the

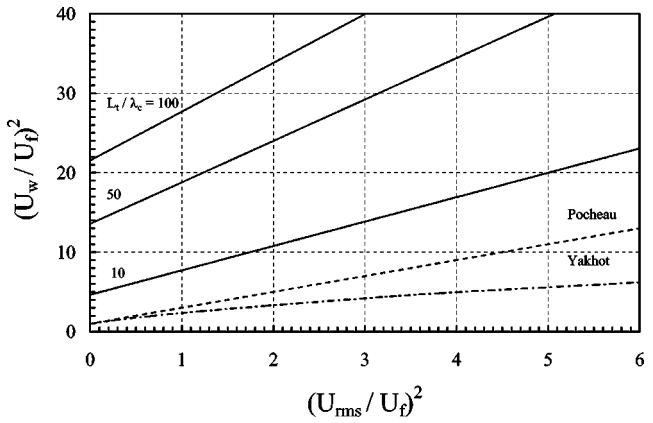

FIG. 1. Scaled flame velocity square $(U_w/U_f)^2$ vs the scaled turbulent velocity square $(U_{rms}/U_f)^2$ for different ratios $\lambda_{max}/\lambda_c=10$, 50, and 100 (solid lines), $L_t=\lambda_{max}$, and $D=1/3$. The dashed and dash-dotted lines show the results by Pocheau [14] and Yakhot [13], respectively.

DL instability working alone without external turbulence. We can see in Fig. 1 that the instability is stronger at larger hydrodynamic length scale allowed by the flow geometry. When turbulent intensity is nonzero, we have an increase in the flame velocity U_w with U_{rms}; and the larger the integral turbulent length scale, the stronger the increase of the flame velocity. This additional dependence of the flame propagation velocity on the turbulent length scale results from the coupling of the DL instability and the external turbulence obtained in the present paper. For comparison, Fig. 1 shows also the turbulent flame velocity predicted by the formulas derived by Pocheau [14], dashed line, and Yakhot [13], dashed-dotted line. Both papers [13,14] developed the renormalization ideas of flame dynamics for the case of zero thermal expansion when $\Theta=1$ and there is no DL instability. The original paper [13] started the approach of scale-invariant flame behavior, but the paper [14] corrected an inconsistency in the analysis of Ref. [13], which led to another formula for the velocity of flame propagation. As we can see, the velocity of flame propagation is much smaller in the case of $\Theta=1$ [14] when the DL instability does not influence flame dynamics. The results of the present paper and Ref. [14] come closer for small values of the maximal hydrodynamic length scale. Still, it is incorrect to think that the results of the present paper go over to the results of Ref. [14] when the hydrodynamic length scale gets smaller. Instead, if the hydrodynamic length scale tends to the cutoff wavelength of the DL instability, $\lambda_{max}\to\lambda_c$ (taking into account $\lambda_{max}\geqslant L_t$), then according to Eq. (53) the velocity of flame propagation tends to the planar flame velocity, $U_w\to U_f$. The rigorous transition from the present theory to the theory of Ref. [14] happens in the limit of small thermal expansion when $\Theta\to 1$ and, consequently, $D\to 0$. In order to investigate such transition, in Fig. 2 we present the velocity of flame propagation versus turbulent intensity for different values of $D=1/6$, 1/3, and 1/2. When $D=0$, the present theory coincides with the theory of Ref. [14]. We have taken $\lambda_{max}/\lambda_c=20$ and $L_t=\lambda_{max}$ in the figure. As we can see in Fig. 2, the larger the fractal excess D provided by the DL

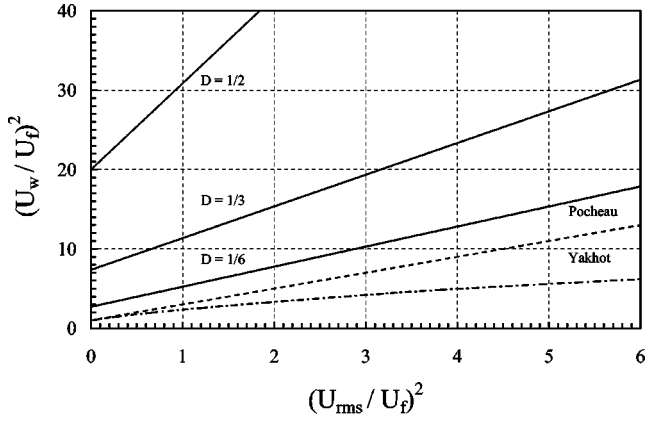

FIG. 2. Scaled flame velocity square $(U_w/U_f)^2$ vs the scaled turbulent velocity square $(U_{rms}/U_f)^2$ for different fractal excess $D=1/6$, 1/3, and 1/2 (solid lines), $\lambda_{max}/\lambda_c=20$, and $L_t=\lambda_{max}$. The dashed and dash-dotted lines show the results by Pocheau [14] and Yakhot [13], respectively.

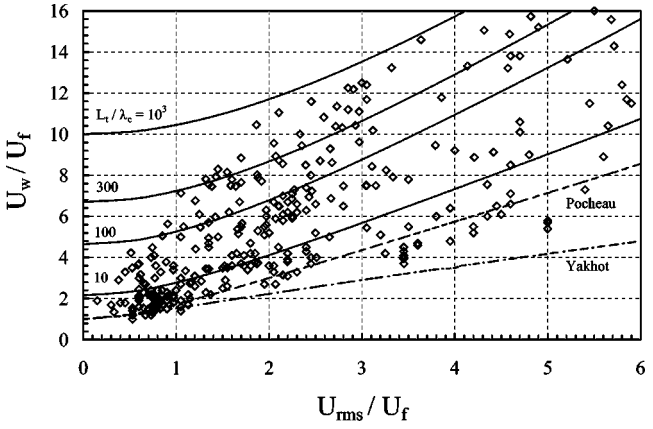

FIG. 3. Scaled flame velocity vs scaled turbulent velocity for different ratios $\lambda_{max}/\lambda_c=10$–$10^3$ (solid lines) with $L_t=\lambda_{max}$. The dashed and dash-dotted lines show the results by Pocheau [14] and Yakhot [13] respectively. The markers show the experimental results [4,8,12].

instability, the larger the velocity of flame propagation. For small values of the fractal excess the plots do tend to the Pocheau result, and this tendency is independent of the integral turbulent length scale.

It is also interesting to compare the present results to the experiments on turbulent flames. In that sense, the most popular experimental publication is a reviewlike paper [4], where a large number of previous experimental results from 36 papers totally have been collected together with the results obtained by the authors of Ref. [4]. The results presented in Ref. [4] have been obtained in different geometries of burning with the characteristic hydrodynamic length scales ranging from several centimeters up to 30 cm of the burning chamber used by the authors of Ref. [4], and even larger. Let us estimate the characteristic values of the ratio λ_{max}/λ_c involved in such experiments. Taking the typical velocity of experimental flames in the range of $U_f=(20$–$200)$ cm/s, we obtain the flame thickness $L_f \simeq \nu/U_f=10^{-3}$–$10^{-2})$ cm. According to the linear theory of the DL instability [1–3,24,25], the typical value of the cutoff wavelength is about $\lambda_c=50L_f$, that is, $\lambda_c=0.05-0.5$ cm, which specifies the characteristic domain for the ratio $\lambda_{max}/\lambda_c=10$–$10^3$. Figure 3 compares the present theoretical results to the experimental results [4]. The theoretical curves are plotted according to Eq. (53) for $D=1/3$, $\lambda_{max}/\lambda_c=10-10^3$, and $L_t=\lambda_{max}$. As we can deduce immediately from Fig. 3, the experimental results do not fall into one curve, but look more like a cloud. Therefore, numerous attempts to describe such a ''cloud'' by one simple formula such as $U_w/U_f=f(U_{rms}/U_f)$, see Ref. [1] as a review, were doomed from the very beginning. Even the Pocheau formula, Eq. (9), which is probably the most mathematically rigorous of the attempts, goes well below the cloud of experimental points. On the contrary, the present analysis includes additional parameters in the dependence of the flame propagation velocity on the turbulent intensity. For this reason, instead of one curve we have a family of curves for different ratios $\lambda_{max}/\lambda_c=10$–$10^3$. As we can see in Fig. 3, for the chosen parameter domain the theoretical curves pass through the middle of the cloud of the experimental points. Such agreement by order of magnitude is encouraging; still, it is difficult to use the results [4] for more detailed quantitative comparison of the theory and the experiments. Different geometries of the experiments included in Ref. [4] demand different theoretical interpretation, and analyzing all of them requires plenty of work and another reviewlike paper such as [4]. Besides, the majority of the experiments included in Ref. [4] have been performed long ago, and the parameters of the turbulent flows such as the integral length scale or even the turbulent intensity involved in the experiments have been often guessed, but not measured.

Instead we will concentrate on one recent experimental paper [34]. The advantage of the experiments [34] for the present comparison is that they have been performed with well-developed turbulent flames propagating in a statistically stationary regime in a tube with a rectangular cross section. The cross-section parameters were 9×3.5 cm^2 with the diagonal 9.7 cm controlling 1/2 of the maximal possible wavelength of the DL instability, λ_{max}. At the same time, according to Ref. [34], the integral turbulent length scale was much lower, $L_t\approx0.5$ cm, so that one has to be careful when applying formulas of the present paper to the experimental conditions of Ref. [34]. The experiment [34] has been performed for propane flames with equivalence ratios $\phi=0.75$, 1, and 1.25. Taking the planar flame velocity and thermal diffusivity ν_{th} for propane flames from Ref. [35] we calculate the respective flame thickness $L_f=\nu_{th}/U_f=8\times10^{-3}$, 4.9×10^{-3}, 5.6×10^{-3} cm. The cutoff wavelength of the DL instability for the propane flames may be evaluated as $\lambda_c/L_f\approx60$, see Ref. [36], and we find $\lambda_c\approx0.48$, 0.29, and 0.34 cm for $\phi=0.75$, 1, and 1.25, respectively. Adopting the turbulent length scale $L_t\approx0.5$ cm in agreement with Ref. [34] we can see that the effect of turbulence should be weak for all equivalence ratios considered, since the parameter L_t/λ_c is close to unity in all three cases $L_t/\lambda_c=1.04$, 1.7, and 1.5. On the contrary, the characteristic hydrodynamic length scale λ_{max} is rather large, $\lambda_{max}/\lambda_c=40.4$, 84.2, and 57.7, and we should expect a noticeable DL instability. Fig-

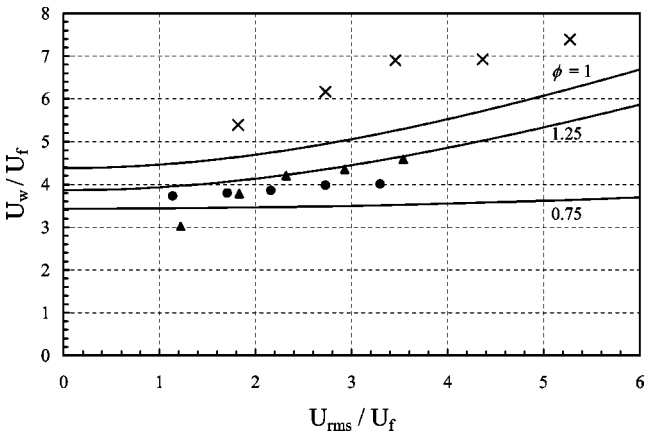

FIG. 4. Scaled flame velocity U_w/U_f vs scaled turbulent velocity U_{rms}/U_f for the experimental configuration [34] with different equivalence ratios $\phi=0.75$, 1, and 1.25 (solid lines). The markers show the experimental results for $\phi=0.75$ (crosses), $\phi=1$ (circles), and $\phi=1.25$ (triangles) [34].

ure 4 compares the theoretical formula, Eq. (53), to the experimental results [34] presented by crosses ($\phi=0.75$), circles ($\phi=1$), and triangles ($\phi=1.25$). As we can see in Fig. 4, in the cases of $\phi=1$, 1.25, the theoretical curves agree rather well with the experimental results both qualitatively and quantitatively. The quantitative difference is within 15–25 %, which may be explained by the experimental errors and inevitable simplifications of the theory. The important property of the experimental points is that for zero turbulent intensity, $U_{rms}=0$, they tend to some velocity of flame propagation, U_w, exceeding the planar flame velocity U_f noticeably. This tendency is especially evident for the stoichiometric flame $\phi=1$, for which the velocity of flame propagation is almost independent of the turbulent intensity and equal to $U_w/U_f=3.75$–4. In the case of $\phi=1.25$ the velocity of flame propagation varies also rather weakly except for one measured point at lower turbulent intensity $U_{rms}/U_f=1.2$. Still, even that point is not far from the theoretical curve. The agreement between the theoretical and experimental results is not so good only for the equivalence ratio $\phi=0.75$, though even in that case we can observe the same qualitative tendencies as for $\phi=1$, 1.25. Particularly, if we extrapolate the experimental points to the case of zero turbulent intensity, then the flame propagation velocity U_w/U_f will be considerably larger than unity, about $U_w/U_f=4$–5. However, unlike the theoretical curve for $\phi=0.75$, the experimental points show noticeable increase of the flame velocity for increasing turbulent intensity. A possible explanation of the disagreement between the theory and the experiment in the case of $\phi=0.75$ is that the integral turbulent length scale has not been, actually, measured in Ref. [34]. Instead, the authors referred to previous measurements for ''a nearly identical burner.'' Still, the integral turbulent length scale is one of the most important parameters in the present theory, and the uncertainty in the experimental value of L_t is crucial for the comparison of the theory and the experiment. Besides, viscous effects influenced the experimental results of Ref. [34] considerably. The condition of no slip at the walls resulted in additional curvature of the flame front, which the authors of Ref. [34] tried to eliminate by phenomenological correction factors to the velocity of flame propagation. The uncertainty in the correction factors may be the other reason for the poor quantitative agreement between the theory and the experiment for $\phi=0.75$. Before the corrections were performed, the experimental points [34] corresponding to different equivalence ratios $\phi=0.75$, 1, and 1.25 were correlated much better. Unfortunately, to the best of our knowledge, so far there has been no theoretical investigation of the DL instability with viscous conditions of no slip at the walls. Therefore at present it is impossible to compare the theory and the experimental points [34] directly as they have been measured without the phenomenological corrections. Finally, if the integral turbulent length scale was indeed as small as it was stated in Ref. [34], that is, $L_t\approx 0.5$ cm, then in the case of $\phi=0.75$ we have an interesting situation when L_t is approximately equal to the cutoff wavelength of the DL instability $L_t\approx\lambda_c$. In that case the multiscaled approach proposed in Ref. [14] and used in the present paper may work for the DL instability, but not for the turbulence-induced terms. On the contrary, in that case finite thickness of the flame front becomes of basic importance for the turbulence-induced solution, since it leads to a resonance at $L_t=\lambda_c$; see Refs. [11,25]. Because of the resonance the coefficient C_t of the turbulence-induced solution may increase considerably, resulting in a much larger velocity of flame propagation, as is shown by the experimental points of Fig. 4.

There is one more interesting point in the comparison of the experimental and theoretical results which should be discussed. The theoretical curves of Figs. 3 and 4 predict a rather large velocity of flame propagation, U_w/U_f, for zero turbulence intensity $U_{rms}/U_f=0$ when the DL instability works alone. The experimental points of Fig. 4, Ref. [34], demonstrate the same tendency. At the same time, the experimental points of Fig. 3, Ref. [4], obviously tend to unity for zero turbulent intensity, $U_w/U_f\rightarrow 1$ for $U_{rms}/U_f\rightarrow 0$. In order to understand this ''contradiction'' we have to take into account the details of the experiments of Ref. [4]. The theoretical curves of Figs. 3 and 4 and the experimental points of Ref. [34] are plotted for a fixed hydrodynamic length scale of the DL instability and a fixed integral length scale of the turbulent flow. On the other hand, the original experiments of Ref. [4] and most of the previous experiments compiled in that paper have been performed for developing flames. In that case flame propagates from a center of a burning chamber, and the turbulent intensity experienced by the flame front in a particular time instant depends on the length scale λ characterizing flame dynamics at that instant. Following the designations of the present paper, such an experiment provides the dependence $U=U(\lambda,u_{rms})$ with $\lambda=\lambda(u_{rms})$ instead of the dependence $U_w=U_w(\lambda_{max},L_t,U_{rms})$ given by Eq. (53) and plotted in Figs. 3 and 4. Then the points with small turbulent intensity correspond to small length scales λ at the beginning of flame propagation, which are much smaller than the maximal integral length scale L_t or the instability length scale λ_{max} allowed by the geometry of the burning chamber. The DL instability is suppressed for these points by thermal conduction and finite flame thickness. As

the flame radius grows, the characteristic length scale of the flame dynamics λ increases and the DL instability develops at the flame front. Besides, the flame interacts with turbulent vortices of a larger size, which implies stronger turbulent intensity. If the integral Reynolds number of the turbulent flow is sufficiently large, then we can present the dependence $U=U(\lambda,u_{rms})$ as a function of the turbulent intensity only using the Kolmogorov spectrum $u_{rms}=U_{rms}(\lambda/L_t)^{1/3}$, or $\lambda=L_t(u_{rms}/U_{rms})^3$. To be particular, we chose the most typical case of $k_t \ll k_c < k_\nu$ and $D=1/3$. Then, according to Eq. (53), the instant velocity of flame propagation depends on the local turbulent intensity as

$$U^2=U_f^2\frac{u_{rms}^2}{U_{rms}^2}\left(\frac{L_t}{\lambda_c}\right)^{2/3}+\frac{4}{3}C_t u_{rms}^2\ln\left(\frac{u_{rms}^3 L_t}{U_{rms}^3\lambda_c}\right) \qquad (54)$$

for $\lambda>\lambda_c$. Besides, $U=U_f$ for $\lambda<\lambda_c$, since the velocity of flame propagation cannot be smaller than the planar flame velocity U_f. It is interesting to note that both the turbulent term and the term related to the DL instability in Eq. (54) are formally proportional to u_{rms}^2. Indeed, the outcome of the DL instability depends on the characteristic length scale λ, which, in turn, is coupled to the turbulent intensity for a developing flame. It is convenient to rewrite the above formula with the help of the parameter

$$\beta=\frac{U_{rms}}{U_f}\left(\frac{\lambda_c}{L_t}\right)^{1/3}. \qquad (55)$$

The introduced parameter compares the planar flame velocity U_f and the turbulent velocity at the length scale equal to the DL cutoff wavelength $U_{rms}(\lambda_c/L_t)^{1/3}$. The parameter β is similar to the Karlovitz number, but it works better in the present studies. Besides, β is unambiguously specified, while the Karlovitz number involves the poorly defined Taylor microscale, which requires extra assumptions and calculations. Following Ref. [4] we may relate the parameter β to the Karlovitz number as $\beta=3.44Ka^{2/3}(\lambda_c/L_f)^{1/3}$, or $\beta=12.7Ka^{2/3}$ in the case of $\lambda_c/L_f=50$ considered in Fig. 3. Then Eq. (54) goes over to

$$U=u_{rms}[\beta^{-2}+4\ln(u_{rms}/\beta U_f)]^{1/2} \qquad (56)$$

for $\lambda>\lambda_c$ and $U=U_f$ for $\lambda<\lambda_c$. Figure 5 presents the dependence, Eq. (56), for the domain $0.07<\beta<1.5$. As we can see in Fig. 5, if we interpret the experimental results as the instant propagation velocity of a developing flame front, then the theoretical curves look quite different from Fig. 3: they start at the planar flame velocity for zero turbulent intensity, and then we have almost linear growth of the flame velocity with turbulent intensity (which depends on the length scale of flame dynamics). Such a shape of the theoretical curves resembles qualitatively the look of clusters of the experimental points selected in Ref. [4] according to the Karlovitz number. In Fig. 5 we have shown different clusters by different markers: crosses for $0.015<\mathrm{Ka}<0.025$ ($0.7<\beta<1$),

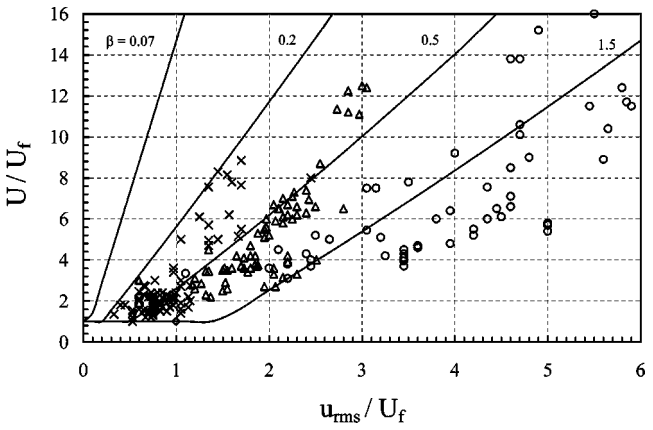

FIG. 5. Scaled flame velocity U/U_f vs scaled local velocity of external turbulence u_{rms}/U_f for a developing flame with $\beta=0.07$–1.5 (solid lines). The markers show the experimental results [4] for $\beta=0.7$–1 (crosses), $\beta=1.6$–1.9 (triangles), and $\beta=3$–4 (circles).

triangles for $0.045<\mathrm{Ka}<0.060$ ($1.6<\beta<1.9$), and circles for $0.12<\mathrm{Ka}<0.17$ ($3<\beta<4$). The experimental points present the velocity of flame propagation with respect to the fuel mixture, which is different from the flame velocity observed in the laboratory reference frame. As we can see in Fig. 5, the smaller the Karlovitz number and the parameter β, the larger the velocity of flame propagation. Such a tendency was pointed out in Ref. [4] on the basis of experimental studies and put in a phenomenological formula for the velocity of flame propagation. The present theory explains this tendency from the first principles. Indeed, if the value of the Karlovitz number (or the parameter β) is small, then the same turbulent intensity is achieved at larger length scales. At the same time larger length scales lead to stronger DL instability and stronger coupling between the instability and the external turbulence, expressed by the factors of the first and second terms in Eq. (53). As a result, we have a larger velocity of flame propagation for smaller values of Ka (or β). Comparing the respective theoretical curves and the clusters of experimental points quantitatively, we can see that the theoretical results go somewhat below the experimental points. However, we would like to remind the reader that the experimental points of Ref. [4] have been collected from a large number of papers involving different experimental configurations. For this reason one cannot expect high accuracy from the quantitative comparison, since different experimental configurations require different interpretations of the theory. Looking at the theoretical curves in Figs. 3 and 5 we can see how large is the difference between these two theoretical interpretations of the experimental results. Usually experiments involve a large number of extra effects, which have not been included in the present theory. For example, the present theory does not take into account the effect of a closed burning chamber used in the original experiments of Ref. [4]. A closed burning chamber results in precompression of the fresh fuel mixture, which increases turbulent intensity and planar flame velocity and decreases flame thickness, thus leading to a larger velocity of turbulent flame propagation.

Flame interaction with acoustic waves is another important effect, which we should expect in a closed burning chamber. As has been pointed out in Refs. [28,36,37], the flame-acoustic interaction may influence the velocity of flame propagation quite strongly damping the DL instability and increasing the effect of the turbulence-induced solution. This indicates that we should be very careful interpreting a particular experiment. For example, it has been questioned in Ref. [38] if the turbulent flames observed in the majority of combustion experiments are statistically stationary, or they present an intermediate asymptotic in the flame dynamics. Strictly speaking, the theoretical results of the present paper consider a statistically stationary turbulent flame, and comparison of the theory with experiments on developing flames may be misleading. Finally, we would like to mention one more limitation of the present theory. In the present paper we have assumed indirectly that the flame is unstable with respect to the DL instability only. An additional thermal-diffusion instability (the Zeldovich instability) [39,40] may reduce the cutoff wavelength λ_c down to the flame thickness and below instead of the large values $\lambda_c=(20-50)L_f$, typical for the DL instability. According to Eq. (53), small values of the cutoff wavelength make the flame instability much stronger, thus increasing the turbulent flame velocity. The effect of noticeably faster propagation of a turbulent flame front affected by the thermal-diffusion Zeldovich instability has been observed in recent experiments [41].

VII. SUMMARY

We have developed the ideas of the self-similar multiscale behavior of a strongly corrugated flame front [14] to the case of a flame influenced both by the external turbulence and by the DL instability. The obtained analytical formulas [with Eq. (53) describing the most typical situation] demonstrate rather strong coupling between external forcing of the flame front by turbulence and intrinsic flame dynamics. The results obtained refute the widely spread idea that the DL instability is of minor importance for the turbulent flames. Instead, the developed theory demonstrates that the DL instability is of principal importance when the characteristic hydrodynamic length scale is large. The case of large hydrodynamic length scales is typical for the majority of combustion configurations corresponding to the flamelet regime of burning. The obtained analytical results agree well with experiments. Still, in order to perform a careful quantitative comparison one has to take into account details of a particular experiment, since even in scope of the same theory we come to quite different formulas for the turbulent flame velocity for different experimental flows, see, for example, Eqs. (53) and (56).

ACKNOWLEDGMENTS

The author is grateful to Derek Bradley and Vyacheslav Akkerman for useful discussions. This work was supported by the Swedish Research Council (VR).

[1] F. A. Williams, *Combustion Theory* (Benjamin, Redwood City, CA, 1985).
[2] P. Clavin, Annu. Rev. Fluid Mech. **26**, 321 (1994).
[3] V. Bychkov and M. Liberman, Phys. Rep. **325**, 115 (2000).
[4] R. Abdel-Gayed, D. Bradley, and M. Lawes, Proc. R. Soc. London, Ser. A **414**, 398 (1987).
[5] Y. Gostintsev, A. Istratov, and Y. Shulenin, Combust., Explos. Shock Waves **24**, 563 (1988).
[6] D. Bradley, T.M. Cresswell, and J.S. Puttock, Combust. Flame **124**, 5551 (2001).
[7] R.C. Aldredge and B. Zou, Combust. Flame **127**, 2091 (2001).
[8] H. Kobayashi, Y. Kawabata, and K. Maruta, in *Proceedings of the 27th Symposium on Combustion*, edited by C. K. Law *et al.* (The Combustion Institute, Pittsburgh, 1998), p. 941.
[9] B. Denet, Phys. Rev. E **55**, 6911 (1997).
[10] N. Peters, H. Wenzel, and F. A. Williams, in *Proceedings of the 28th Symposium on Combustion*, edited by C. K. Law *et al.* (The Combustion Institute, Pittsburgh, 2000), p. 235.
[11] M. Zaytsev and V. Bychkov, Phys. Rev. E **66**, 026310 (2002).
[12] R.C. Aldredge, V. Vaezi, and P.D. Ronney, Combust. Flame **115**, 395 (1998).
[13] V. Yakhot, Combust. Sci. Technol. **60**, 191 (1988).
[14] A. Pocheau, Phys. Rev. E **49**, 1109 (1994).
[15] V. Akkerman and V. Bychkov, Combust. Theory Modelling (to be published).
[16] P. Clavin and F.A. Williams, J. Fluid Mech. **90**, 589 (1979).
[17] V. Bychkov, K. Kovalev, and M. Liberman, Phys. Rev. E **60**, 2897 (1999).
[18] O. Travnikov, V. Bychkov, and M. Liberman, Phys. Rev. E **61**, 468 (2000).
[19] V. Bychkov, Phys. Fluids **10**, 2091 (1998).
[20] V. Bychkov, S. Golberg, M. Liberman, and L.E. Eriksson, Phys. Rev. E **54**, 3713 (1996).
[21] S. Kadowaki, Phys. Fluids **11**, 3426 (1999).
[22] A.R. Kerstein, W.T. Ashurst, and F.A. Williams, Phys. Rev. A **37**, 2728 (1988).
[23] G. Sivashinsky, Acta Astronaut. **4**, 1177 (1977).
[24] P. Pelce and P. Clavin, J. Fluid Mech. **124**, 219 (1982).
[25] G. Searby and P. Clavin, Combust. Sci. Technol. **46**, 167 (1986).
[26] V. Bychkov, Phys. Rev. Lett. **84**, 6122 (2000).
[27] V. Bychkov (unpublished).
[28] V. Bychkov, Phys. Rev. Lett. **89**, 168302 (2002).
[29] S. Ishizuka, Prog. Energy Combust. Sci. **28**, 477 (2002).
[30] L. D. Landau and E. M. Lifshitz, *Fluid Mechanics* (Pergamon Press, Oxford, 1989).
[31] A. Ungut, A. Gorgeon, and I. Gokalp, Combust. Sci. Technol. **92**, 265 (1993).
[32] O.L. Gulder and G.J. Smallwood, Combust. Flame **103**, 107 (1995).
[33] G.J. Smallwood *et al.*, Combust. Flame **101**, 461 (1995).
[34] T. Lee and S. Lee, Combust. Flame **132**, 492 (2003).
[35] S. Davis, J. Quinard, and G. Searby, Combust. Flame **130**, 123 (2002).
[36] G. Searby and D. Rochweger, J. Fluid Mech. **231**, 529 (1991).

[37] V. Bychkov, Phys. Fluids **11**, 3168 (1999).
[38] A.N. Lipatnikov and J. Chomiak, Prog. Energy Combust. Sci. **28**, 1 (2002).
[39] G.I. Barenblatt, Ya.B. Zeldovich, and A.G. Istratov, Prikl. Mekh. Tekh. Fiz. **2**, 21 (1962).
[40] Ya. B. Zeldovich *et al.*, *The Mathematical Theory of Combustion and Explosion* (Consultants Bureau, New York, 1985).
[41] K.T. Aung, M.I. Hassan, S. Kwon, L.K. Tseng, O.C. Kwon, and G.M. Faeth, Combust. Sci. Technol. **174**, 61 (2002).